



**HAL**  
open science

## Metal-organic vapor phase epitaxy of BInGaN quaternary alloys and characterization of boron content

Simon Gautier, Gaëlle Orsal, Tarik Moudakir, N. Maloufi, François Jomard, Marc Alnot, Zakaria Djebbour, Andrei Sirenko, M. Abid, K. Pantzas, et al.

► **To cite this version:**

Simon Gautier, Gaëlle Orsal, Tarik Moudakir, N. Maloufi, François Jomard, et al.. Metal-organic vapor phase epitaxy of BInGaN quaternary alloys and characterization of boron content. *Journal of Crystal Growth*, 2010, 312 (5), pp.641-644. 10.1016/j.jcrysgro.2009.11.040 . hal-00554242

**HAL Id: hal-00554242**

**<https://hal.science/hal-00554242>**

Submitted on 5 Jul 2022

**HAL** is a multi-disciplinary open access archive for the deposit and dissemination of scientific research documents, whether they are published or not. The documents may come from teaching and research institutions in France or abroad, or from public or private research centers.

L'archive ouverte pluridisciplinaire **HAL**, est destinée au dépôt et à la diffusion de documents scientifiques de niveau recherche, publiés ou non, émanant des établissements d'enseignement et de recherche français ou étrangers, des laboratoires publics ou privés.



Distributed under a Creative Commons Attribution - NonCommercial 4.0 International License

# Metal-organic vapour phase epitaxy of BInGaN quaternary alloys and characterization of boron content

S. Gautier<sup>a,\*</sup>, G. Orsal<sup>a</sup>, T. Moudakir<sup>b</sup>, N. Maloufi<sup>c</sup>, F. Jomard<sup>d</sup>, M. Alnot<sup>e</sup>, Z. Djebbour<sup>f,g</sup>, A.A. Sirenko<sup>h</sup>, M. Abid<sup>i</sup>, K. Pantzas<sup>i</sup>, I.T. Ferguson<sup>j</sup>, P.L. Voss<sup>i</sup>, A. Ougazzaden<sup>i</sup>

<sup>a</sup> Laboratoire Matériaux Optiques, Photonique et Système (LMOPS), UMR CNRS 7132, University of Metz and Supelec, 2 rue E. Belin, F-57070 Metz, France

<sup>b</sup> UMI 2958 Georgia Tech-CNRS, 2-3 rue Marconi, 57070 Metz, France

<sup>c</sup> Laboratoire d'Etude des Textures et Application aux Matériaux, FRE CNRS 3143, University of Metz, ISGMP, Ile du Saulcy, F-57012 Metz, France

<sup>d</sup> Laboratoire de Physique des Solides et de Cristallogénèse (LPSC), UMR 8635 CNRS, University of Versailles-Saint-Quentin1, place Aristide Briand, 92195 Meudon Cedex, France

<sup>e</sup> Laboratoire de Physique des Matériaux, UMR CNRS 7556, Université Henri Poincaré, Bd des aiguillettes B.P. 239, F-54506 Vandoeuvre les Nancy, France

<sup>f</sup> Laboratoire de Génie Electrique de Paris, UMR 8507 CNRS, SUPELEC, University Paris-Sud 11, University Pierre et Marie Curie, 11 rue Joliot Curie, 91192 Gif-sur-Yvette, France

<sup>g</sup> Department of Physics and Engineering Science, University of Versailles UVSQ, 45 Av. Des Etats Unis, 78035 Versailles, France

<sup>h</sup> Department of Physics, New Jersey Institute of Technology, Newark, NJ 07102, USA

<sup>i</sup> Georgia Institute of Technology/GT-Lorraine-UMI 2958 Georgia Tech-CNRS, 2-3 rue Marconi, 57070 Metz, France

<sup>j</sup> School of Electrical and Computer Engineering, Georgia Institute of Technology, Atlanta, GA 30332, USA

BInGaN quaternary alloys with up to 2% boron and 14% of indium have been grown on GaN/sapphire template substrates by metal-organic vapour phase epitaxy (MOVPE). Epitaxial layer composition was determined by secondary ion mass spectroscopy (SIMS), and confirmed by X-ray photoelectron spectroscopy (XPS). Bandgap energies were measured using optical transmission and reflection spectroscopy. We find that boron incorporation in BInGaN reduces the bandgap, causing an effect similar to the increase of indium content in InGaN. However, adding boron has the advantage of decreasing the lattice mismatch with conventional GaN substrates.

## 1. Introduction

The InGaN system covers a broad range of wavelengths from UV (3.4 eV for GaN) [1] to infrared (0.7 eV for InN) [2]. As a result, InGaN has been extensively studied and commercialized for solid-state light sources in the green/blue/violet spectral regions. InGaN will also extend the functionality of a wide range of optoelectronic devices for photovoltaics [3], medical diagnostics, and full color displays [4]. Many groups have studied InGaN structures including quantum wells and quantum dots to realize such devices. However, for high indium content, the lattice mismatch between the InGaN layer and the GaN template substrates causes high misfit dislocation densities, limiting the range of indium composition.

One solution to this problem is the addition of boron in order to decrease the lattice mismatch of InGaN with respect to a GaN substrate. For instance, an alloy containing 3% boron decreases

the lattice mismatch of  $\text{In}_{0.15}\text{Ga}_{0.85}\text{N}/\text{GaN}$  by 0.6%. BInGaN quaternary alloys offer the possibility to optimize the bandgap energy and lattice parameter independently of each other without inducing strain into the layers. This is highly desirable for the bandgap engineering of advanced optoelectronic heterostructures [5]. In addition, the incorporation of boron into GaN-based devices will potentially allow the development of a new class of neutron detectors [6]. In this paper we report on the epitaxial growth and characterization of BInGaN materials for optoelectronic and neutron detection applications.

## 2. Experiment

Growth was performed in a low pressure MOVPE T-shape reactor using only nitrogen as a carrier gas [7]. Trimethylgallium (TMGa), trimethylindium (TMIn), triethylboron (TEB) III-group precursors were used as gallium, indium, and boron sources, respectively. For the MOVPE growth of InGaN-based materials, a relatively low growth temperature is essential to ensure In incorporation and due to the inefficient decomposition of  $\text{NH}_3$  a

\* Corresponding author. Tel.: +33 3 87 37 85 40, fax: +33 3 87 37 85 59.  
E-mail address: simon.gautier@metz.supelec.fr (S. Gautier).

very large flow rate of  $\text{NH}_3$  is required [8]. In this study, dimethylhydrazine (DMHy) precursor was added because of its low decomposition temperature which enhances the concentration of atomic nitrogen in the gas phase, allowing the growth at a relatively low flow rate of  $\text{NH}_3$  at the growth temperature of  $730^\circ\text{C}$  [9]. However, adding high flow rates of DMHy leads to undesirable carbon deposition in the growth chamber. In this study, the optimum value of the DMHy/V ratio was around 4%. As a result, no parasitic reaction in the vapour phase between DMHy and (TMIn, TMGa) was observed. The In incorporation in the solid phase was found to be proportional to the TMIn/III ratio in the vapour phase and the growth rate values were as expected.

A large number of BInGaN samples have been grown, however this work focuses on a systematic series of three samples in which the flow of TMGa and TMIn was constant to investigate boron incorporation in these samples. The TEB flow was varied between 0, 3.27, and 6.54 sccm leading to a TEB/III molar ratio in the vapour phase of 0%, 2%, and 4%, respectively.

Our growth chamber has been designed to provide good thickness uniformity over 2" wafers. Strain uniformity across the wafers has been investigated for each boron concentration given above. So far, BInGaN alloys have been grown on multipieces of  $2\text{ cm}^2$  template substrates in the same run and no significant shift of the HR-XRD peaks has been observed on samples from the same run.

A typical structure consists of a 40 nm GaN buffer layer grown on GaN template substrate, followed by a 140 nm BInGaN layer.

### 3. Results and discussion

Lattice parameters of BInGaN layers were measured by high resolution X-ray diffraction (HR-XRD) including symmetrical and asymmetrical  $2\theta-\omega$  scans, and both symmetrical and asymmetrical reciprocal space mapping (RSM). Surface topography and RMS roughness were investigated by atomic force microscopy (AFM) in intermittent contact mode. Secondary ion mass spectroscopy (SIMS) was used to obtain the depth concentration profile for Ga, In, B, N, and impurities such as O, etc. The bandgap energy was obtained by optical absorption measurements. The composition measurement of quaternary BInGaN is not straightforward because of the relatively low boron content in these samples. Therefore a baseline was created using ternary alloys of InGaN and BGaN of various indium and boron contents, measured

with a high accuracy by HR-XRD, and used as reference to calibrate SIMS for quantitative measurements of boron and indium in the BInGaN layers. The BInGaN composition results were later confirmed by X-ray photoelectron spectroscopy (XPS) measurements.

Fig. 1 shows (00.2)  $2\theta-\omega$  scans of BInGaN layers grown with various TEB flows. The peak at lower angle and of lower intensity corresponds to the BInGaN film whereas the other peak at higher angle corresponds to diffraction from the GaN template. The signal from the GaN template dominates the X-ray diffraction profile since the GaN layer is  $3.5\ \mu\text{m}$  thick compared to 140 nm for the BInGaN. At increased TEB flow, the peak corresponding to BInGaN shifts towards the GaN peak indicating a reduction of the misfit strain. The RSMs of the asymmetric (11.4) plane show fully relaxed BInGaN layers, as presented in Fig. 2(a and b). At boron percentage of 0% and based on Vegard's law the average In content in the ternary InGaN reference layer was equal to 19.5%.

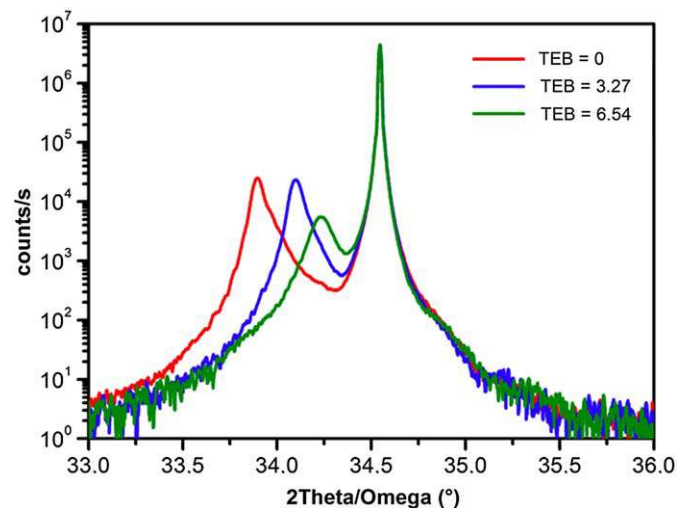


Fig. 1.  $2\theta-\omega$  symmetric HRXRD scans showing the GaN, InGaN and BInGaN (00.2) diffraction peaks for various TEB flows.

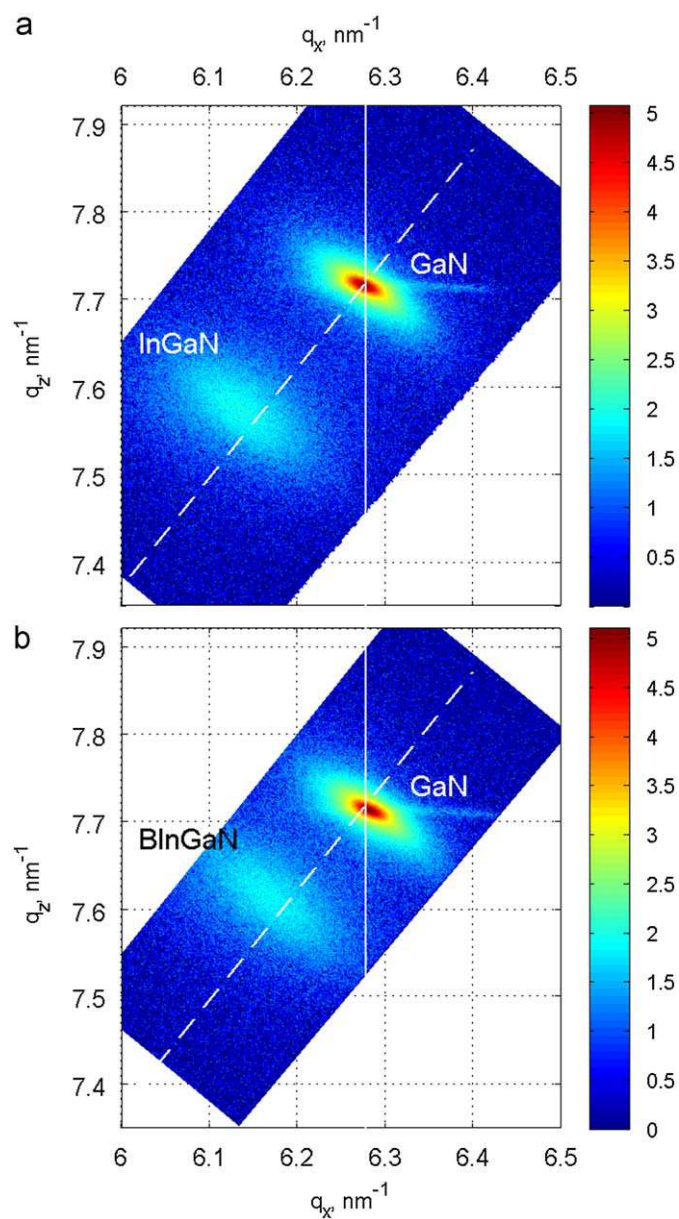


Fig. 2. Reciprocal space maps of the (11.4) diffraction of the InGaN and BInGaN samples grown on GaN template for (a) TEB=0 sccm and (b) TEB=3.27 sccm. Both samples demonstrate the complete relaxation of strain between the grown layer and the GaN substrate.

Atomic force microscopy showed that the BInGaN surface exhibits morphology similar to that reported for InGaN [10] and RMS roughness was between 3 and 5 nm.

The SIMS profile exhibits a uniform boron distribution (Fig. 3) in the BInGaN layer, along the growth direction, while the Ga concentration varies anti-phase with the In and B. This is an indication that the mixing of In, Ga, and B atoms occurs on the sub-lattice of III sites to form an alloy. Depth concentration profile analysis of In, Ga, B and N concentrations were also performed by SIMS for all samples. As mentioned above, several B<sub>x</sub>GaN and InGaN layers were used as reference in order to calibrate SIMS analysis for quantitative measurements of boron and indium content in the BInGaN layers. It was found that an increase of the TEB flow in the growth chamber from 0 to 6.54 sccm lead to a B and In content variation in the solid phase from 0% to 2% and from 19.5% to 14%, respectively.

XPS analysis was performed for all samples to further understand these results. Broad range and elemental XPS spectra were measured using Al K $\alpha$  X-ray and Mg K $\alpha$  X-ray sources to avoid the overlaps with Auger lines. The binding energies were charge-corrected by referencing the C 1s to 285.00 eV. The composition,

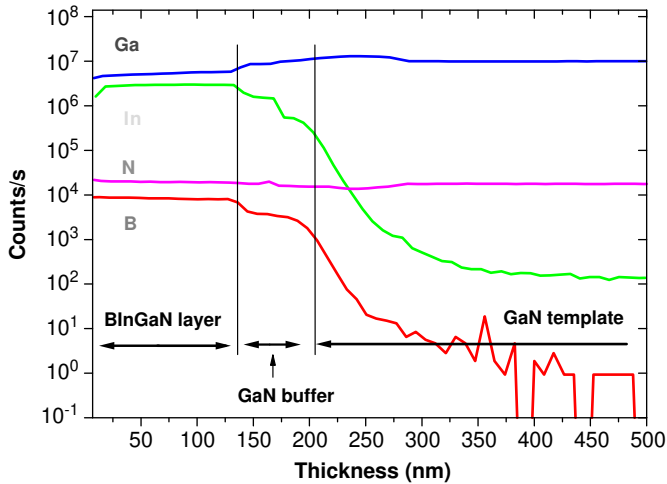


Fig. 3. SIMS elemental concentration depth profiles for the B, In, Ga and N signals for the BInGaN on GaN template.

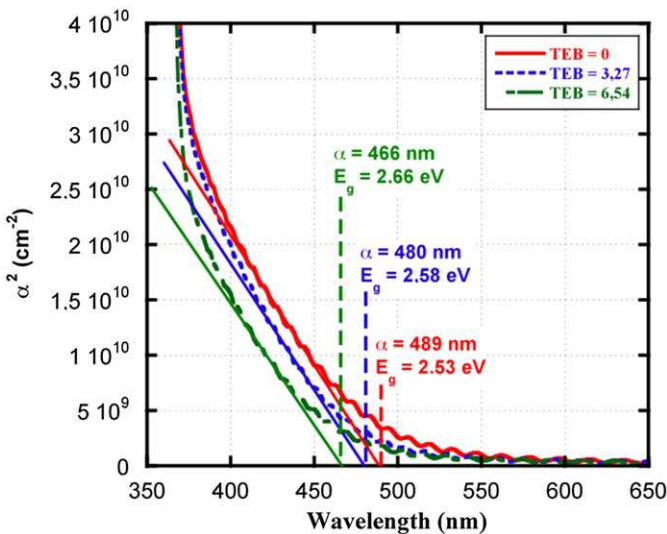


Fig. 4. Optical absorbance versus wavelength for three BInGaN samples.

both boron and indium, obtained by XPS and SIMS are in good agreement.

Optical spectroscopy was utilized to investigate the bandgap variation in the BInGaN layers. Transmission  $T(\lambda)$  and reflection  $R(\lambda)$  spectra versus the wavelength were measured at room temperature with a Perkin Elmer LAMBDA 950 spectrophotometer. Absorbance spectra  $\alpha^2(\lambda)$  are shown in Fig. 4. They have been obtained from transmission and reflection data as  $\alpha(\lambda) = (1/d) \times \ln\{[1 - R(\lambda)]/T(\lambda)\}$ ,  $d$  being the thickness of the BInGaN layers. The extrapolation of the linear section of  $\alpha^2$  to zero absorption corresponds to the optical bandgap, which is illustrated in the same figure for these three samples. These bandgap values are shown as data points (a), (b), and (c) in Fig. 5, which plots bandgap versus the out-of-plane lattice parameter.

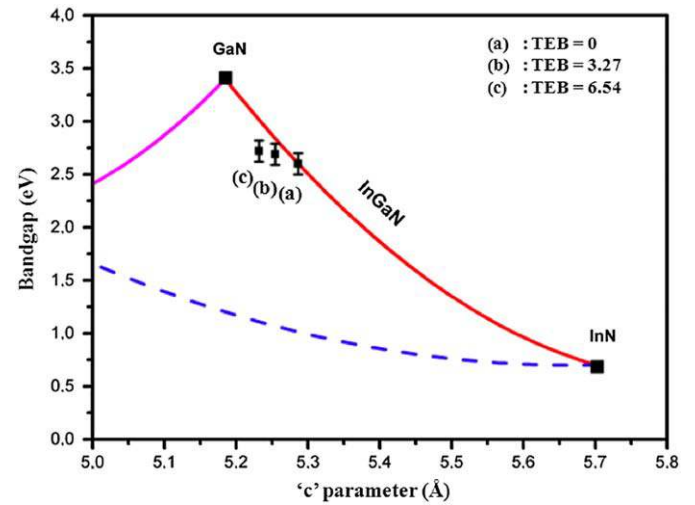


Fig. 5. Bandgap energy versus out-of-plane lattice parameter  $c$  for nitride compounds. Experimental data are shown with squares.

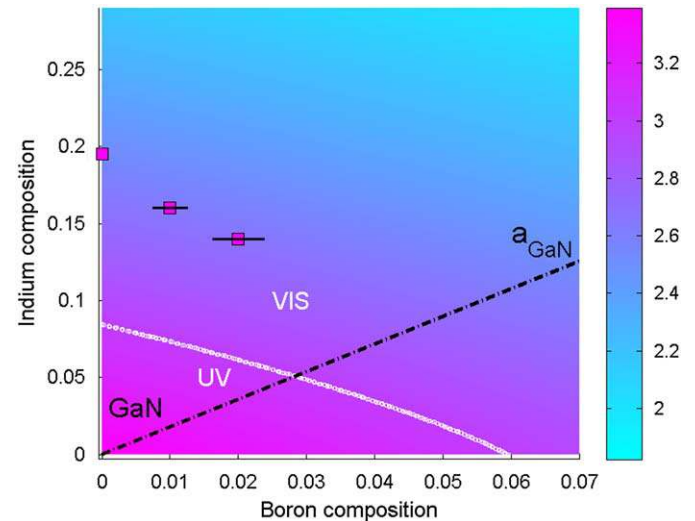


Fig. 6. Calculated bandgap values for quaternary  $B_xIn_yGa_{1-x-y}N$  compound. The low-left corner corresponds to the binary endpoint of GaN. The straight line that originates from the GaN corner corresponds to the  $(x,y)$  compositions that are lattice matched to the in-plane lattice parameter of GaN. The white curve corresponds to the  $B_xIn_yGa_{1-x-y}N$  bandgap of 3 eV and divides the UV and visible parts of the corresponding optical spectrum. Experimental points for three  $B_xIn_yGa_{1-x-y}N$  samples are shown with squares. The size of the squares in vertical direction corresponds to the uncertainty of the indium composition. The horizontal error bars indicate the uncertainty in the measured boron composition.

Fig. 6 shows calculated bandgap values for quaternary  $B_xIn_yGa_{1-x-y}N$  compound, which have been obtained using equations and the bandgap values of the endpoint binaries (GaN, InN, BN) from Refs. [11–15]:  $E_g(\text{GaN})=3.39$  eV,  $E_g(\text{BN})=5.5$  eV, and  $E_g(\text{InN})=0.7$  eV. The bowing parameter  $C_{\text{BGaN}}=9.2$  eV of the BGaN ternary compound is from Ref. [16]. To accommodate our experimental value of 2.53 eV for the bandgap of  $In_{0.195}Ga_{0.805}N$  sample, the bowing parameter of InGaN was chosen to be  $C_{\text{InGaN}}=2.1$  eV, which is 10% less than the recommended value of 2.3 eV from Ref. [14]. Since our experimental data and the  $\{x,y\}$  range for the calculated bandgap values are close to the GaN binary endpoint, the bowing parameter of BInN has practically no influence on the calculated values shown in Fig. 6. We were using  $C_{\text{BInN}}=14$  eV, which was obtained by extrapolating the dependence of the bowing parameters in ternary nitride compounds as a function of the lattice mismatch between the binary endpoints. Note that BInN should have the highest value of the bowing parameters among all known ternary nitrides since boron and indium have the highest contrast in the III-nitrogen bonding length [16].

Two experimental values for  $B_{0.01}In_{0.16}Ga_{0.83}N$  and  $B_{0.02}In_{0.14}Ga_{0.84}N$  samples are shown in Fig. 6. Within the error bars of the boron composition, the measured bandgaps of  $B_xIn_yGa_{1-x-y}N$  compounds are in a perfect agreement with the calculated values, thus confirming the strong effect of the bandgap bowing in this quaternary system. It is notable that a combination of the two bowing parameters for ternary compounds of InGaN and BGaN results in a decrease of the bandgap for BInGaN quaternary compound, which is lattice matched to GaN for a broad range of the  $x$  and  $y$  compositions (see straight line in Fig. 6). In other words, the addition of boron to InGaN has an effect similar to that of increased indium for the bandgap decrease. At the same time, in terms of the lattice parameter this quaternary compound demonstrates a decrease of the lattice mismatch with respect to GaN. It opens a possibility to design, for example, light emitters for the green and yellow parts of the visible spectrum with the  $B_xIn_yGa_{1-x-y}N$  active region that is lattice matched to conventional GaN substrates.

#### 4. Conclusion

We demonstrate the growth of a new quaternary alloys BInGaN, with boron content up to 2% at indium content of 14%. These materials have the potential to allow independent choice of bandgap and lattice parameter for bandgaps between 0.7 and 3.4 eV, enabling advanced III-N heterostructure designs. Our experimental results confirm a strong bowing for the bandgap of the quaternary system of BInGaN with  $C_{\text{InGaN}}=2.1$  eV and  $C_{\text{BGaN}}=9.2$  eV.

#### References

- [1] W.G. Perry, T. Zheleva, M.D. Bremser, R.F. Davis, W. Shan, J.J. Song, J. Electron. Mater. 26 (1997) 224.
- [2] J. Wu, W. Walukiewicz, K.M. Yu, J.W. Ager III, E.E. Haller, H. Lu, W.J. Schaff, Y. Saito, Y. Nanishi, Appl. Phys. Lett. 80 (2002) 3967.
- [3] O. Jani, I. Ferguson, C. Honsberg, S. Kurtz, Appl. Phys. Lett. 91 (2007) 132117.
- [4] S. Nakamura, S. Pearton, G. Fasol, in: The Blue Laser Diode, Springer, Berlin, 2000.
- [5] T. Kimura, T. Matsuoka, Jpn. J. Appl. Phys. 46 (2007) L574.
- [6] J. Uher, S. Pospisil, V. Linhart, M. Schieber, Appl. Phys. Lett. 90 (2007) 124101.
- [7] S. Gautier, C. Sarte, S. Ould-Saad, J. Martin, A. Sirenko, A. Ougazzaden, J. Cryst. Growth 298 (2007) 428.
- [8] F.K. Yam, Z. Hassan, Superlattices Microstructures 43 (2008) 1.
- [9] T. Moudakir, G. Orsal, N. Maloufi, S. Gautier, M. Bouchaour, T. Aggerstam, S. Ould Saad, J.P. Salvestrini, A. Ougazzaden, Eur. Phys. J. Appl. Phys. 43 (2008) 295.
- [10] M. Gartner, C. Kruse, M. Modreanu, A. Tausendfreund, C. Roder, D. Hommel, Appl. Surf. Sci. 253 (2006) 254.
- [11] S.L. Romyantsev, M.E. Levinshtein, A.D. Jackson, S.N. Mohammad, G.L. Harris, M.G. Spencer, M.S. Shur, in: Properties of Advanced Semiconductor Materials GaN, AlN, InN, BN, SiC, SiGe, Wiley, New York, 2001, pp. 67–92.
- [12] V. Bougrov, M.E. Levinshtein, S.L. Romyantsev, A. Zubrilov, in: Properties of Advanced Semiconductor Materials GaN, AlN, InN, BN, SiC, SiGe, Wiley, New York, 2001, pp. 1–30.
- [13] I. Vurgaftman, J.R. Meyer, L.R. Ram-Mohan, J. Appl. Phys. 89 (2001) 5815.
- [14] M. Hori, K. Kano, T. Yamaguchi, Y. Saito, T. Araki, Y. Nanishi, N. Teraguchi, A. Suzuki, Phys. Status Solidi (b) 234 (2002) 750.
- [15] T. Matsuoka, H. Okamoto, M. Nakao, H. Harima, E. Kurimoto, Appl. Phys. Lett. 81 (2002) 1246.
- [16] A. Ougazzaden, S. Gautier, T. Moudakir, Z. Djebbour, Z. Lochner, S. Choi, H.J. Kim, J.-H. Ryou, R.D. Dupuis, A.A. Sirenko, Appl. Phys. Lett. 93 (2008) 083118.